

## On the application of a dynamic-stochastic climate model to the simulation of the oceanic upper layer thermal variability

OLEG O. RYBAK

*Scientific Research Centre of the Russian Academy of Sciences,  
8-a Theatralnaya St., Sochi, Krasnodar Region, 354000 Russia*

(Manuscript received Sept. 30, 1991; accepted in final form Jan. 16, 1992)

### RESUMEN

Un modelo dinámico-estocástico basado en el modelo termodinámico del clima de Adem con forzamiento aleatorio es considerado. Se propone una forma simplificada para incluir el balance de agua. Los campos computados de las desviaciones estándares de las anomalías de temperatura mensuales de la capa mezclada oceánica y de las anomalías mensuales del flujo turbulento de calor son bastante realistas. La introducción de anomalías de la advección por corrientes de deriva producidas por el viento y de anomalías del flujo de calor latente resultan ser las fuentes más importantes de la variabilidad de la capa superior oceánica. Modelos de autorregresión de las anomalías mensuales de la capa mezclada oceánica se discuten.

### ABSTRACT

A dynamic-stochastic model based on random forcing of Adem thermodynamic climate model is considered. The way of including simplified atmospheric water budget is proposed. Computed fields of standard deviations of ocean mixed layer monthly temperature anomalies and turbulent heat flux monthly anomalies are quite realistic. Inputs of the anomalies of the wind drift currents advection and anomalies of latent heat flux are found to be the most important sources of the upper ocean layer variability. Autoregressive models of the ocean mixed layer monthly anomalies are discussed.

### 1. Introduction

The analysis of climatological research tendencies (Nicolis and Prigogine, 1990) has already made clear the governing trends in modern climatology. One of them is the climatic simulation with the help of advanced Global Circulation Models (GCM). This trend has always been associated with the development of supercomputers and computational algorithms. The second one assumes, to a great extent, a qualitative attitude to climatological problems. In order to follow this way an explorer needs an efficient tool to manage with complicated climate system with enormous number of feed-backs and numerous exchange processes. This "phenomenological" approach has been a reason for various rather simple climatic models to be desired as some sort of alternatives to GCM. Simple climate models (such as Budyko-Sellers type or any other energy-balance model or the thermodynamic model suggested by Adem) have proved to be undoubtedly useful in constructing the principles of interactions inside the climatic system.

Stochastic climate theory (Hasselmann, 1976) has provided new approaches for simple climate models constructions and applications (a brief review of Monte Carlo simulation using Adem's thermodynamic model can be found in Dobrovolski *et al.* (1991).

Now we present, in an advanced version, a Dynamic-Stochastic Model (DSM). Our aim is to include a simplified pattern of hydrological cycle into a DSM and give an example of evaluation of different inputs into the total variability of any part of the climate system.

## 2. Model description

The methods of Sea Surface Temperature(SST) variability simulation by means of stochastic forcing of a thermodynamic model were discussed in Dobrovolski *et al.* (1991). Mid-tropospheric monthly temperature anomalies were assumed to be “weather variables” (using Hasselmann’s terminology). One of the shortages of this approach is the impossibility to simulate the tropospheric layer variability, because it is considered to be a white noise process according to definition. Another shortage is the lack of complete evidence that the tropospheric layer thermal variability can adequately be reproduced by thermal variability at the middle of the layer (in the statistical sense). These two reasons made us to look for alternative “weather variables” for DSM.

The current version assumes four random “weather variables” to force the heat conservation equations for tropospheric and oceanic layers and the water vapour conservation equation. These variables are: the zonal and the meridional wind speed components at the 850 mb surface, the evaporation from the surface of the ocean (or continent) and the cloud cover. The reasons for the 850 mb surface to be chosen instead of the surface corresponding to the mid-tropospheric height were discussed by Dobrovolski *et al.* (1991).

The system of heat conservation equations can be obtained, for example, from Adem (1979). We use these equations to compute monthly anomalies of the variables.

For the tropospheric layer:

$$\frac{\partial T'_m}{\partial t} + AD_m - K_m \nabla^2 T'_m = (E'_T + G'_2 + G'_5)/H_m \quad (1)$$

For the Ocean Mixed Layer (OML):

$$\frac{\partial T'_s}{\partial t} + AD_s - K_s \nabla^2 T'_s = (E'_s - G'_2 - G'_3)/H_s \quad (2)$$

For the continental layer:

$$E'_T - G'_2 - G'_3 = 0 \quad (3)$$

The following notation is used in equations (1) to (3):

$T'_s$  -mid-tropospheric monthly temperature anomaly;

$T'_m$  -OML monthly temperature anomaly;

$G'_2$  -sensible heat flux monthly anomaly;

$G'_3$  -latent heat flux monthly anomaly;

$G'_5$  -monthly anomaly of the heat flux from the condensation in the cloud layer;

$E'_T$  -monthly anomaly of the radiation heat flux to the tropospheric layer;

$E'_s$  -monthly anomaly of radiation heat flux to the Earth surface;

$H_s = \rho_s c_s h_s$ ,  $H_m = c_v a_o$ , where

$\rho_s$  -sea water specific weight;

$c_s$  -sea water specific heat;

$h_s$  -mixed layer depth;

$c_v$  -air specific heat at constant volume;

$a_o$  -weight of tropospheric layer unit.

$K_s$  and  $K_m$  -large scale horizontal turbulence coefficients,

$K_s = 3 \times 10^8$  and  $K_m = 3 \times 10^{10}$  ( $\text{cm}^2 \text{sec}^{-1}$ ) (see Adem, 1979);

$AD_s$  -advection of heat by the anomaly of the wind drift currents;

$AD_m$  -advection of heat by climatological mean wind.

$$AD_s = V'_x \frac{\partial T'_{Ns}}{\partial x} + V'_y \frac{\partial T'_{Ns}}{\partial y}, \quad (4)$$

$$AD_m + U_{Nx} \frac{\partial T'_m}{\partial x} + U_{Ny} \frac{\partial T'_m}{\partial y}, \quad (5)$$

where  $V'_x$  and  $V'_y$  are the zonal and the meridional components of the anomaly of the wind drift currents computed according to Adem (1979),  $T'_{Ns}$  is the SST climatological field (Metodicheskiye materyaly ... , 1977),  $U_{Nx}$  and  $U_{Ny}$  are the climatological zonal and meridional wind components (Atlas ... , 1975).

The equations for parameterization of heating functions  $E'_T$ ,  $E'_s$  and  $G'_2$  from Adem (1979), are used. We only have to transform them in order that monthly anomalies of  $E_T$ ,  $E_s$  and  $G_2$  are only left:

$$E'_T = A''_2 T'_m + (A_3 + (\epsilon_N + \epsilon') D_3) T'_s + \epsilon' (D'_6 + b_3 I) \quad (6)$$

$$E'_s = B''_2 T'_m + B_3 T'_s + \epsilon' (B_7 + (k - 1)(1 - \alpha)(Q + q)_o) \quad (7)$$

$$G'_2 = K_3 U (T'_m - T'_s) \quad (8)$$

where  $A''_2$ ,  $A_3$ ,  $B''_2$ ,  $B_3$ ,  $B_7$ ,  $D_3$ ,  $D'_6$ ,  $b_3$ ,  $k$ ,  $K_3$  are constants (see Adem, 1964),  $\alpha$  is the surface albedo (Henderson-Sellers and Wilson, 1983),  $\epsilon_N$  is the cloud cover climatic zonal means and  $U$  is computed according to the following expression:

$$U = \left\{ (U_{Nx} + U'_x)^2 + (U_{Ny} + U'_y)^2 \right\}^{\frac{1}{2}} \quad (9)$$

$U'_x$  and  $U'_y$  are monthly anomalies of  $U_{Nx}$  and  $U_{Ny}$ .

We describe  $G'_3$  as series of random fields with a given monthly and spatial standard deviation and space correlation structure, both being obtained from observed data. Standard deviation fields  $\sigma(G'_3)$  over the North Atlantic for February and August are taken from Androushenko *et al.* (1987). The values for the rest of the months are approximated by the following simple expression:

$$\sigma(G'_3)_i = \sigma(G'_3)_{i=2} \cos^2 \{(i - 2)\pi/12\} + \sigma(G'_3)_{i=8} \sin^2 \{(i - 2)\pi/12\}, \quad (10)$$

where  $i$  is the month number.

For continental regions  $\sigma(G'_3)$  fields are computed from observed data. We use only the time series of 11 water balance stations in the USSR European Territory because of lack of information from the rest of the continental regions. In the arid zones, corresponding to desert and semideserts, zero evaporation anomalies are assumed.

Standard deviations of cloud cover monthly anomalies  $\sigma(\epsilon')$  are considered to be constant (Jarosh, 1986),  $\sigma(\epsilon') = 0.1$ .

Standard deviation of wind components monthly anomalies  $\sigma(U'_x)$  and  $\sigma(U'_y)$  were taken from Atlas ... (1975) and interpolated from grid  $10^\circ \times 10^\circ$  into grid  $5^\circ \times 5^\circ$ .

Spatial correlation of any random field is adequate to the observed one.

Spatial correlation for  $U'_x$  and  $U'_y$  is considered to be that of monthly anomalies of water vapour transport fields on 850 mb surface (Jarosh, 1986). Spatial correlation for  $G'_3$  fields was estimated from the corresponding time series of Ocean Weather Stations (OWS) "A", "C", "D", "I" and "M". OWS data were obtained from Ariel *et al.* (1984). Cloud cover anomalies are considered to be spatially uncorrelated.

The last equation to be included into the system is the water vapour conservation equation, written for monthly anomalies also:

$$\frac{\partial Q'}{\partial t} + \frac{\partial F'_x}{\partial x} + \frac{\partial F'_y}{\partial y} = E' - P' \quad (11)$$

where:

$Q'$  -monthly anomaly of the total precipitable water;

$F'_x$  -monthly anomaly of the zonal component of the total water vapour flux;

$F'_y$  -monthly anomaly of the meridional component of the total water vapour flux;

$E'$  -monthly anomaly of the evaporation rate;

$P'$  - monthly anomaly of the precipitation rate.

It is natural to consider  $G'_3 = LE'$  and  $G'_5 = LP'$ , where  $L$  is the specific heat of condensation. Now one can easily express  $G'_5$  from formula (11).

It was shown by Dobrovolski *et al.* (1991) how to compute  $F'_x$ ,  $F'_y$  and  $Q'$  using 850 mb data:

$$F'_x = K_x F'_{x850} \quad (12)$$

$$F'_y = K_y F'_{y850} \quad (13)$$

$$Q' = K_q a'_{850} \quad (14)$$

where  $K_x$ ,  $K_y$  and  $K_q$  are the empirical coefficients estimated from observations;  $F'_{x850}$  and  $F'_{y850}$  are the zonal and the meridional components of the water vapour flux at 850 mb;  $a'_{850}$  is monthly anomaly of the air absolute humidity at 850 mb.

$$F'_{x850} = a'_{850} U_{Nx} + a_{N850} U'_x \quad (15)$$

$$F'_{y850} = a'_{850} U_{Ny} + a_{N850} U'_y \quad (16)$$

where  $a_{N850}$  is a normal value of the air absolute humidity at 850 mb. Both  $a_{N850}$  and  $a'_{850}$  are computed using the technique suggested by Adem (1967).

The algorithms for the model integration do not vary essentially from those described by Adem (1965). The length of numerical experiments was 120 months.

### 3. Results of the OML variability simulations

To compare the results of the OML simulation with the observed sea surface temperature (SST) variability it is useful to compute standard deviation fields of simulated time series with the corresponding fields of observed SST as for example in Metodicheskiye materiyaly ... (1977). Standard deviation of the OML monthly anomalies, computed for the case when it is being forced by all inputs (anomalies of the wind drift currents, anomalies of sensible and latent heat fluxes and anomalies of radiation heating) and mixed layer depth  $h_s = 25$  m, are shown on the Figures 1 (January) and 2 (July).

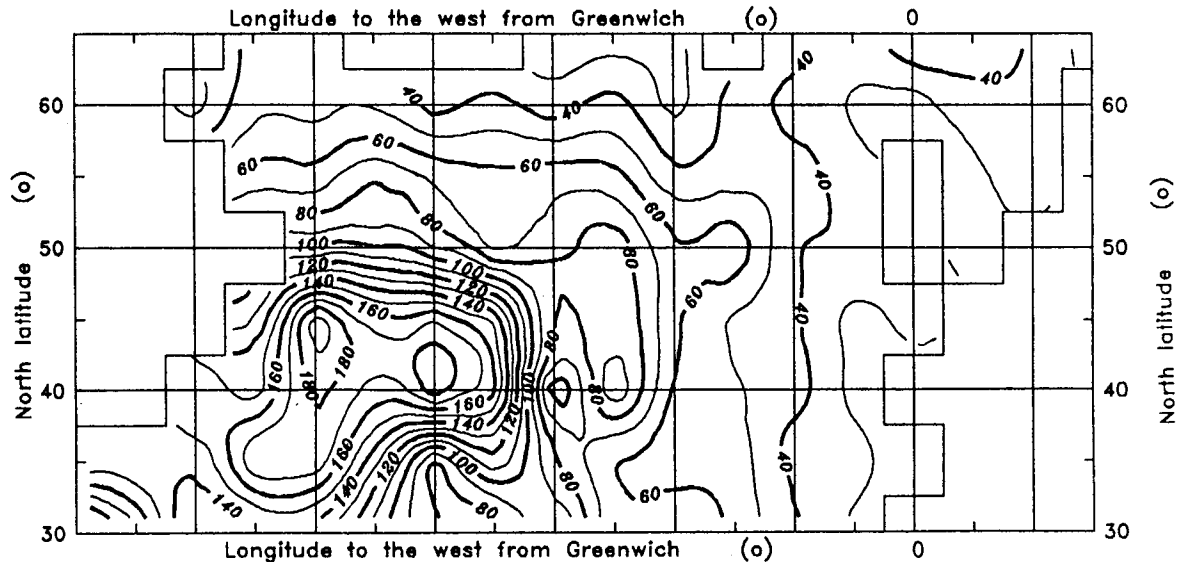


Fig. 1. Standard deviation of the mixed ocean layer monthly temperature anomalies (in hundredth of degrees Celsius). North Atlantic. January.

To evaluate the individual inputs one can carry out the experiments when the model is driven by only one of them and then compare the fields of variances of the outputs. The results of such comparison are shown in Figures 3 to 6. There are some interesting details to point out. The inputs of latent heat flux anomalies and anomalies of the wind drift currents produce the largest part of output variance. These two variance sources do not change essentially over the region from winter to summer. Input of anomalies of wind drift currents prevails in those parts of the region where gradients of climatic SST values are strong, those are zones of oceanic fronts. Anomalies of latent heat flux play a more noticeable role in rather "quite" regions, which are in the south of the model integration region, where climatic SST gradients are negligibly small.

It is rather difficult to evaluate the inputs of anomalies of sensible and radiant heat fluxes because they are quite insignificant in comparison with the ones discussed. Their inputs into

the total variance do not exceed the confidential intervals for the period of integration of 120 months.

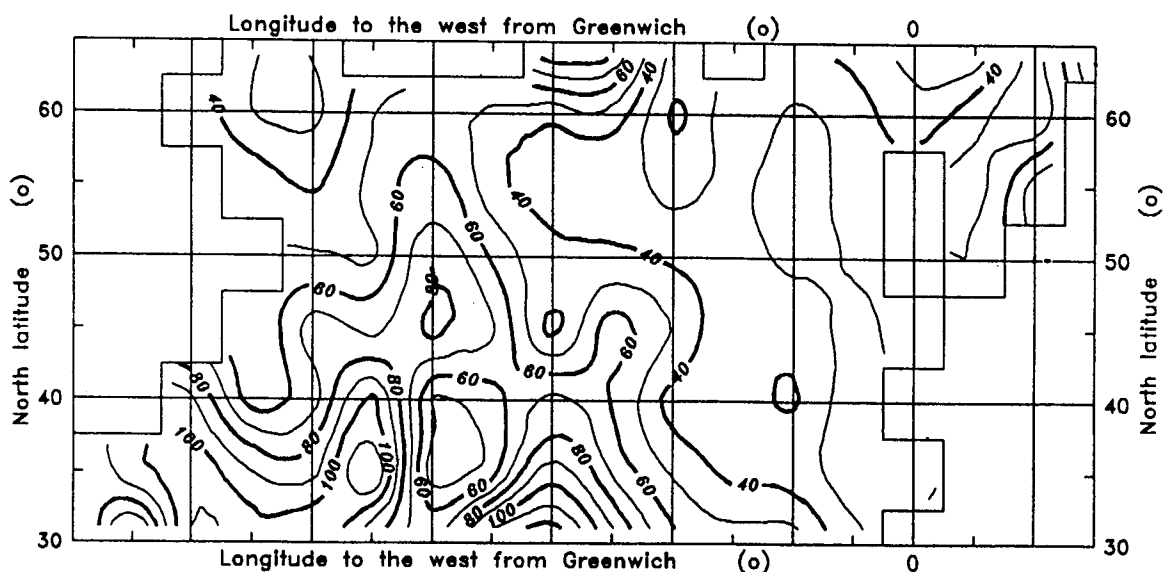


Fig. 2. Standard deviation of the mixed ocean layer monthly temperature anomalies (in hundredth of degrees Celsius). North Atlantic. July.

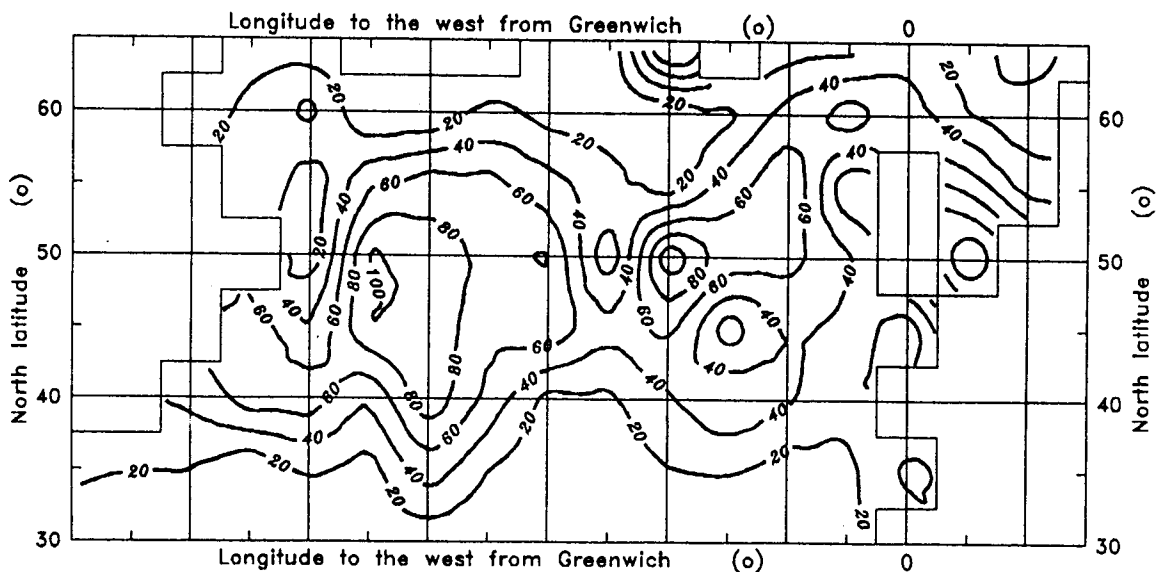


Fig. 3. Relation (in percent) of the variance of the ocean mixed layer monthly temperature anomalies caused by the anomalies of the wind drift currents to the variance caused by all forcing sources. North Atlantic. January.

The standard deviation of sensible heat flux monthly anomalies has also been computed (Figs. 7, 8). One can compare them with those computed by Androushenko *et al.* (1987). The computed field for July is rather smooth. In contrast the January field has strong gradients, with a maximum in regions adjacent to frontal zones.

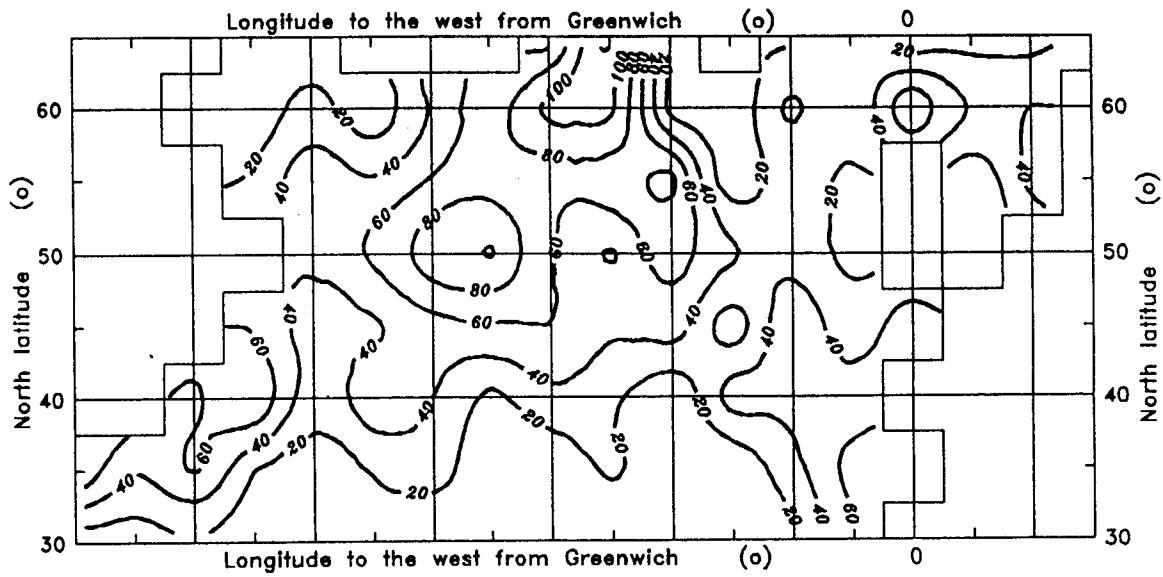


Fig. 4. Relation (in percent) of the variance of the ocean mixed layer monthly temperature anomalies caused by the anomalies of the wind drift currents to the variance caused by all forcing sources. North Atlantic. July.

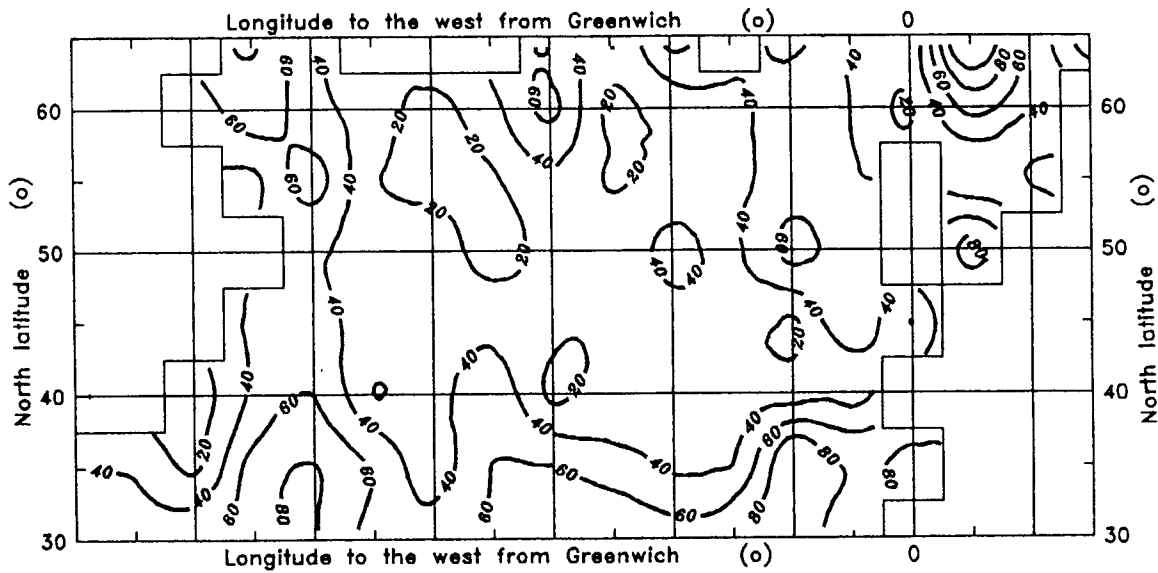


Fig. 5. Relation (in percent) of the variance of the ocean mixed layer monthly temperature anomalies caused by the anomalies of latent heat flux to the variance caused by all forcing sources. North Atlantic. January.

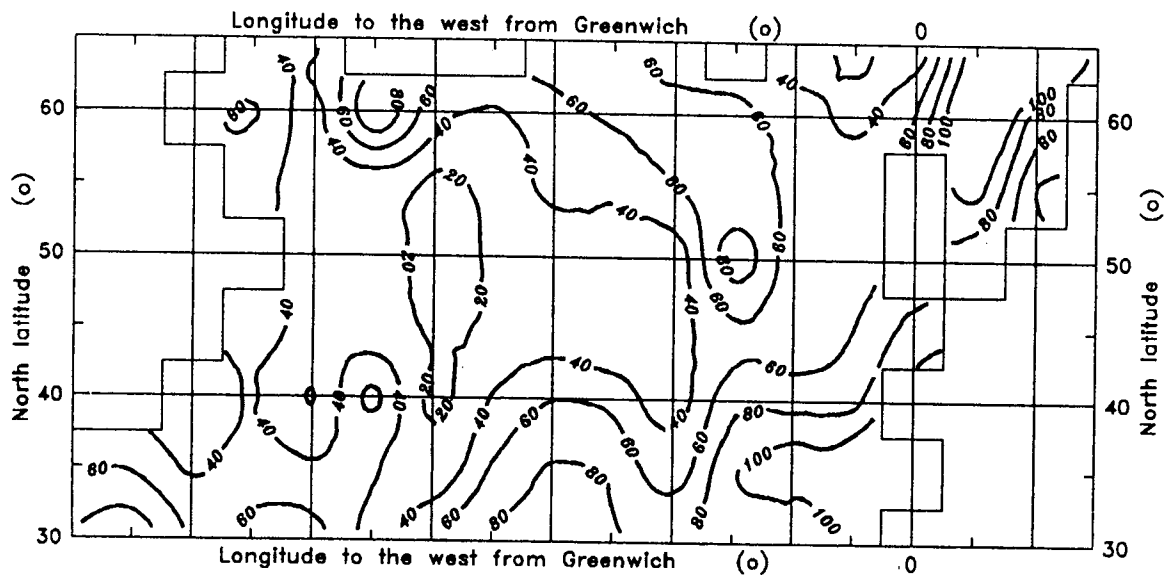


Fig. 6. Relation (in percent) of the variance of the ocean mixed layer monthly temperature anomalies caused by the anomalies of latent heat flux to the variance caused by all forcing sources. North Atlantic. July.

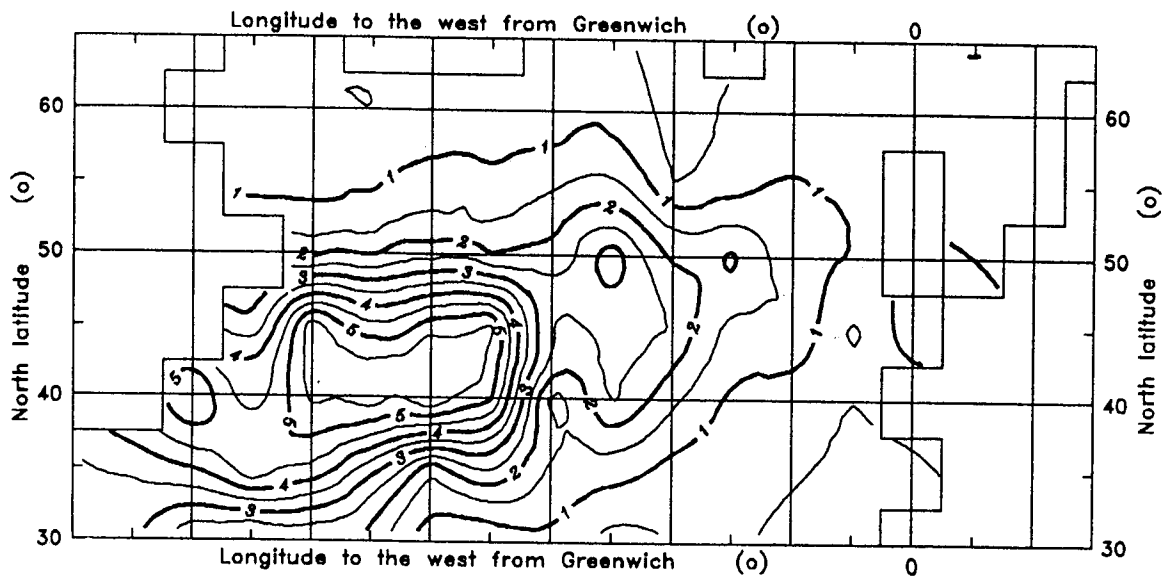


Fig. 7. Standard deviation of sensible heat flux monthly anomalies ( $\text{MJ} \times \text{m}^{-2} \times \text{day}^{-1}$ ). North Atlantic. January.



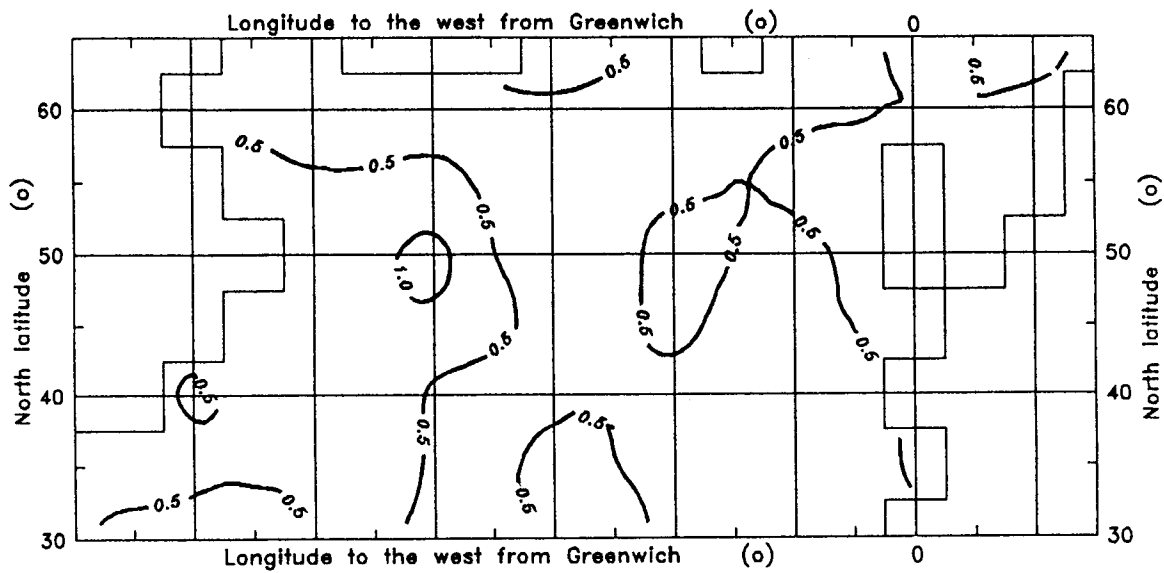


Fig. 8. Standard deviation of sensible heat flux monthly anomalies ( $\text{MJ} \times \text{m}^{-2} \times \text{day}^{-1}$ ). North Atlantic. July.

**4. Autoregressive models of the OML monthly anomalies**

The Burg-Levinson method was used to compute autoregressive (AR) models of order 1 – 4 for model-generated time series. Optimal AR order was chosen according to Parzen criterium (CAT). FORTRAN programs of autoregressive analysis were designed by Privalsky (1985).

The chart of AR optimal order for OML monthly anomalies is shown in Figure 9. The largest part (65%) of the time series is best fitted with the first order AR models. This result does not contradict the hypothesis of Hasselmann (1976) stating the red spectrum of “climatic variables”

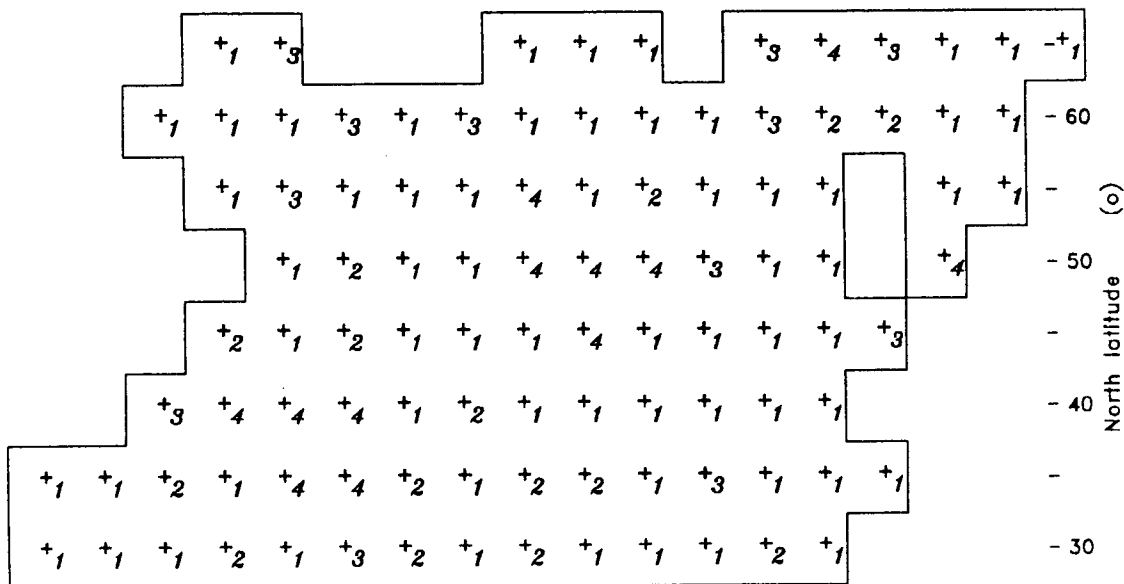


Fig. 9. Autoregressive models optimal orders (fourth is maximal) for the North Atlantic ocean mixed layer monthly temperature anomalies. Crosses are located in  $5^\circ \times 5^\circ$  grid points.

(such as OML) as a reply to stochastic forcing. It is quite noticeable that there is no considerable differences between the AR coefficients of order 1 ( $A_{1,1}$ ) and first AR coefficients of the optimal order ( $A_{1,n}; n = 1, \dots, 4$ ). One can see this fact from the three-dimensional diagram in Figure 4. The greatest part of the integration region (more than 80%) enjoys the approximate equality of  $A_{1,1}$  and  $A_{1,n}$  excluding several gaps in the south and projections in the north and south-east where  $|A_{1,n} - A_{1,1}| \geq 0.2$ . Residual in other areas does not exceed the confidence intervals for AR coefficients estimates. So one can assert that climatic variability of OML may be described

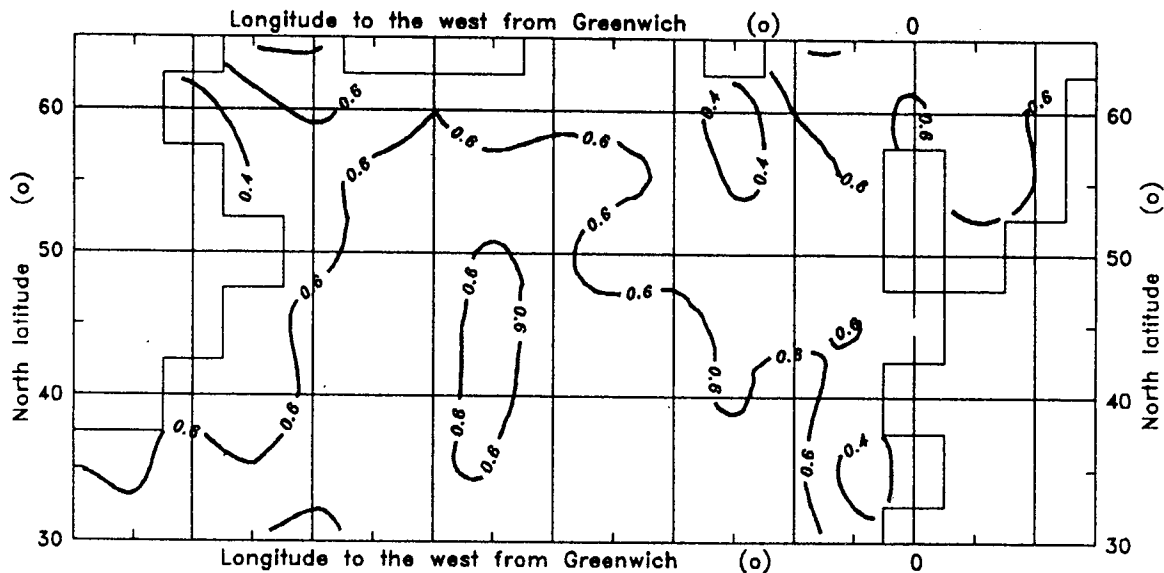


Fig. 10. First-order AR model coefficients (correlation coefficients with one-month lag) for the ocean mixed layer monthly temperature anomalies.

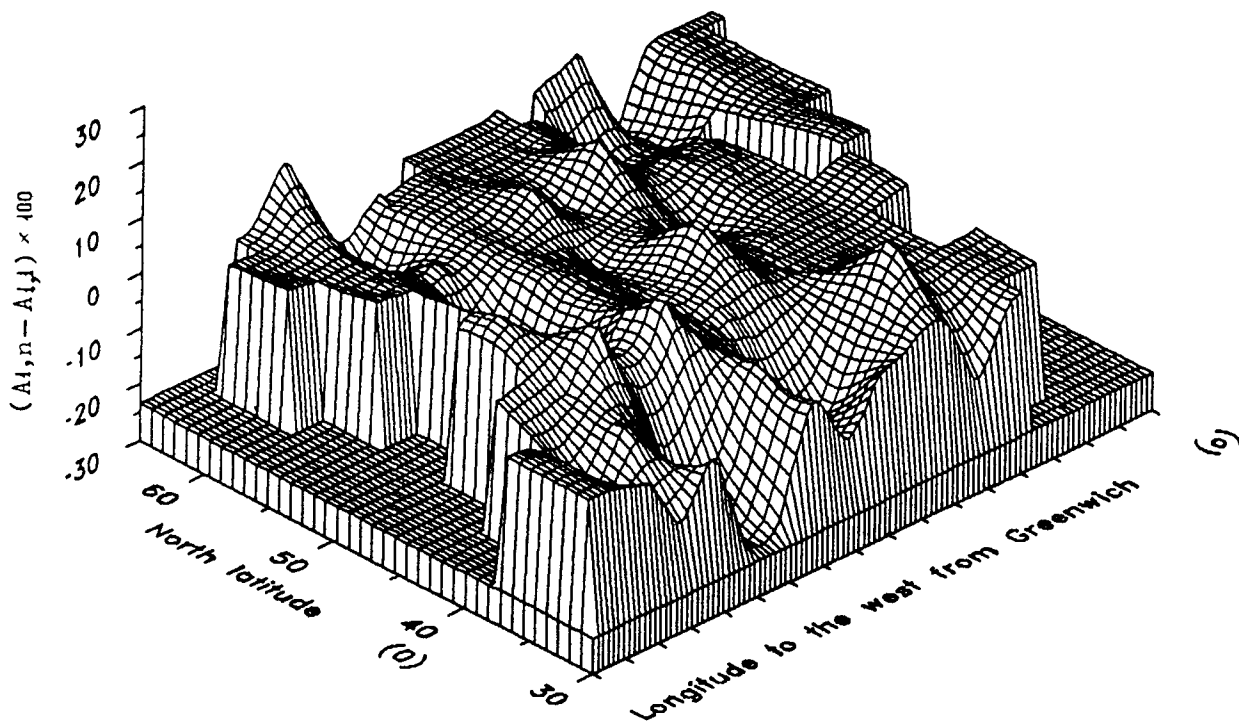


Fig. 11. Difference between  $A_{1,n}$  (first coefficient of the AR model of the optimal order  $n = 1, \dots, 4$ ) and  $A_{1,1}$  (coefficient of the AR model of order 1). AR coefficients were computed for the time series of the North Atlantic ocean mixed layer monthly temperature anomalies, generated in the numerical experiments with the dynamic-stochastic model.

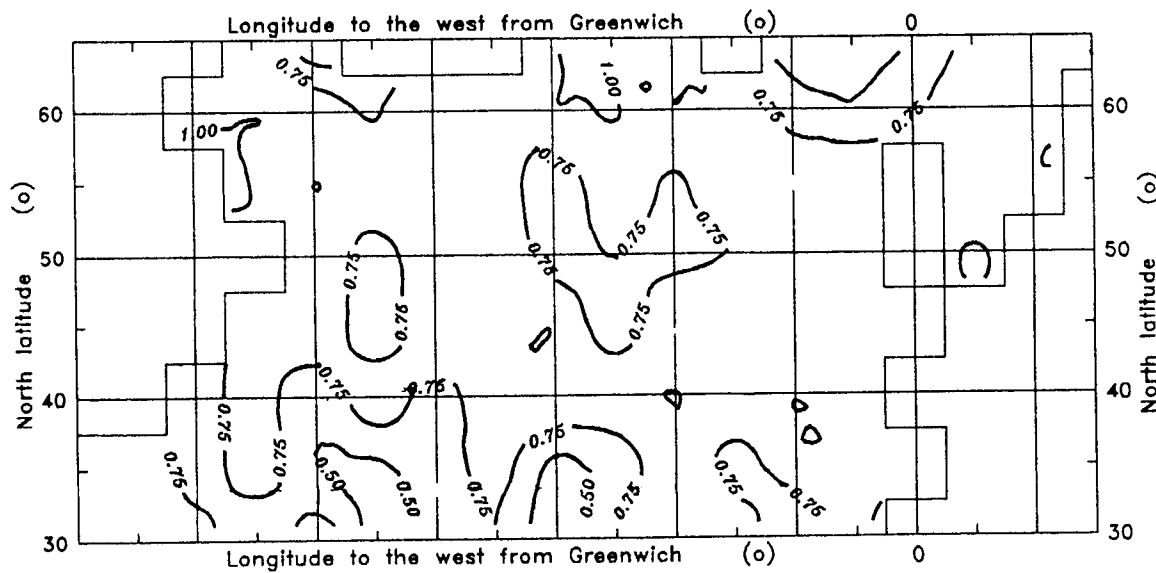


Fig. 12. White noise variance for the ocean mixed layer monthly temperature anomalies AR models of order 1 - 4.

by the first order AR models (simple Markov chain) in a large part of the North Atlantic. Chart of  $A_{1,1}$  is shown in Figure 10. Values of  $A_{1,1} = 0.5 \div 0.7$  prevail over region (60% of the model time series). White noise variance field is shown in Figure 12. It is obvious that the regions with low white noise variance are located in the north-east and the south-west where its values do not exceed 0.75.

## 5. Concluding remarks

The current version of the dynamic-stochastic model has obviously proved to be able to reproduce the main features of OML variability in the climatic time scale. Stochastic features of the model generated and observed fields are quite alike excluding the regions located to a large extent in rather narrow zones of oceanic fronts.

We can point the resembling work of Blaauboer *et al.* (1982) where the OML variability for the North Sea is simulated also from the standpoint of stochastic climate theory. The OML was forced by the random sensible and latent heat fluxes. Red spectrum of the OML monthly variability has been obtained. North Pacific SST variability was explored by Reynolds (1978). He found out that the SST variability can be simulated by low-order AR models with exception of regions of strong oceanic currents.

The author's point of view is that the obvious advantage of Adem type models (both in their pure dynamic or dynamic-stochastic variants) is their physical clearness. One can rather easily trace the transformation of any perturbation in the complicated mechanisms of climatic variability and to explain to himself the physical background of the chain of alterations caused by one or another disturbances in the external (like the Earth's orbital parameters) or internal forcing mechanisms. The GCM do not provide an opportunity of such rather inexpensive testing.

## REFERENCES

- Adem, J., 1964. On the physical basis for the numerical prediction of monthly and seasonal temperature in the troposphere-ocean-continent system. *Mon. Wea. Rev.*, **92**, 91-103.

- Adem, J., 1965. Experiments aiming of monthly and seasonal numerical weather prediction. *Mon. Wea. Rev.*, **93**, 495-503.
- Adem, J., 1967. Parameterization of atmospheric humidity using cloudiness and temperature. *Mon. Wea. Rev.*, **95**, 83-88.
- Adem, J., 1979. Low resolution thermodynamic grid models. *Dyn. Atmos. Oceans.*, **3**, 433-451.
- Androushenko, J. N., Z. N. Ariel and I. I. Ivanova, 1987. 'Izmenchivost srednemesyahnykh znacheniy kharakteristik energoobmena okean-atmosfera v Severnoy Atlantike' (Variability of monthly mean values of the energy exchange parameters in the North Atlantic). *Chief Geophysics Observatory Publishers, Leningrad, Gidrometeoizdat*, N 506, 93-107 (in Russian).
- Ariel, Z. N., B. N. Yegorov and I. I. Ivanova, 1984. 'Kharakteristiki energoobmena okean-atmosfera' (Ocean-atmosphere energy exchange data). Leningrad, *Gidrometeoizdat*, 80 p. (in Russian).
- 'Atlas klimaticheskikh kharakteristik temperatury, plotnosty i davleniya vozdukh, vetra i gheopotentsiala v troposfere i nizhney stratosfere Severnogo polusharya' (The atlas of climatic data on air temperature, density and pressure, wind and geopotential heights in the troposphere and lower estratosphere of the Northern Hemisphere). Ed. by D. I. Stekhnovsky and I. V. Khanevskaya. Leningrad, *Gidrometeoizdat*, 1975 (in Russian).
- Blaauboer, D., G. J. Komen and J. Reiff, 1982. The behaviour of sea surface temperature (SST) as a response to stochastic latent and sensible heat forcing. *Tellus*, **34**, 17-28.
- Dobrovolski, S. G., O. O. Rybak and J. S. Jarosh, 1991. Construction of dynamic-stochastic heat and water exchange climate models using the approach of J. Adem. *Geofis. Int.*, **30**, 5-12.
- Hasselmann, K., 1976. Stochastic climate models. Part 1. Theory. *Tellus*, **28**, 473-485.
- Henderson-Sellers, A. and M. F. Wilson, 1983. Surface albedo data for climate modelling. *Rev. Geophys. Space Phys.*, **21**, 1743-1788.
- Jarosh, J. S., 1986. 'Issledovaniye sezonnikh anomalij kharakteristik atmosfernoj vetvi gidrologicheskovo tsikla (na primere territorii SSSR)' (On the seasonal anomalies of the hydrologic cycle atmospheric branch (on the USSR territory primarily). Cand. Sci (Geography) Thesis. Moscow, 1986 (in Russian).
- 'Metodicheskiye materyaly k gidrometeorologicheskoy kharakteristike promyslovykh rayonov Severnoy Atlantiky' (Methodical materials for the hydrometeorological feature of fishery regions of the North Atlantic). Part 1, Sea surface temperature anomalies in 1957-1971. Kaliningrad. *Fisheries and Oceanography Scientific Research Institute Publishers*, 1977, 92 p. (in Russian).
- Nicolis, G. and I. Prigogine, 1990. 'Poznanye slozhnogo' (Understanding the complicity). Moscow, *Mir*, 344 p. (in Russian).
- Privalsky, V. E., 1985. 'Klimaticheskaya izmenchivost. Stokhasticheskiye modeli, predskazuemost, spectry' (Climatic variability. Stochastic models, predictability, spectra). Moscow, *Nauka*, 180 p. (in Russian).
- Reynolds, R. W., 1978. Sea surface temperature anomalies in the North Pacific Ocean. *Tellus*, **30**, 97-103.